Atmos. Chem. Phys. Discuss., 9, 1977–2020, 2009
www.atmos-chem-phys-discuss.net/9/1977/2009/

Atmospheric Chemistry and Physics Discussions

This discussion paper is/has been under review for the journal *Atmospheric Chemistry and Physics (ACP)*. Please refer to the corresponding final paper in *ACP* if available.

Evaluation of CLaMS, KASIMA and ECHAM5/MESSy1 simulations in the lower stratosphere using observations of Odin/SMR and ILAS/ILAS-II

F. Khosrawi[1,*], R. Müller[1], M. H. Proffitt[2], R. Ruhnke[3], O. Kirner[3], P. Jöckel[4], J.-U. Grooß[1], J. Urban[5], D. Murtagh[5], and H. Nakajima[6]

[1]ICG-1, Forschungszentrum Jülich, 52425 Jülich, Germany
[2]Proffitt Instruments, 1109 Havre Lafitte Drive, Austin, Texas 78746, USA
[3]IMK, Forschungszentrum Karlsruhe, 76021 Karlsruhe, Germany
[4]MPI for Chemistry (Otto Hahn Insitute), 55128 Mainz, Germany
[5]Dept. of Radio and Space Science, Chalmers Univ. of Technology, 41296 Göteborg, Sweden
[6]NIES, Tsukuba, Ibaraki, 305-8506 Japan
[*]now at: MISU, Stockholm University, 10691 Stockholm, Sweden

Received: 15 October 2008 – Accepted: 17 November 2008 – Published: 22 January 2009

Correspondence to: F. Khosrawi (farah@misu.su.se)

Published by Copernicus Publications on behalf of the European Geosciences Union.

Abstract

1-year data sets of monthly averaged nitrous oxide (N_2O) and ozone (O_3) derived from satellite measurements were used as a tool for the evaluation of atmospheric photochemical models. Two 1-year data sets, one derived from the Improved Limb Atmospheric Spectrometer (ILAS and ILAS-II) and one from the Odin Sub-Millimetre Radiometer (Odin/SMR) were employed. Here, these data sets are used for the evaluation of two Chemical Transport Models (CTMs), the Karlsruhe Simulation Model of the Middle Atmosphere (KASIMA) and the Chemical Lagrangian Model of the Stratosphere (CLaMS) as well as for one Chemistry-Climate Model (CCM), the atmospheric chemistry general circulation model ECHAM5/MESSy1 (E5M1) in the lower stratosphere with focus on the Northern Hemisphere. Since the Odin/SMR measurements cover the entire hemisphere, the evaluation is performed for the entire hemisphere as well as for the low latitudes, midlatitudes and high latitudes using the Odin/SMR 1-year data set as reference. To assess the impact of using different data sets for such an evaluation study we repeat the evaluation for the polar lower stratosphere using the ILAS/ILAS-II data set. Only small differences were found using ILAS/ILAS-II instead of Odin/SMR as a reference, thus, showing that the results are not influenced by the particular satellite data set used for the evaluation. The evaluation of CLaMS, KASIMA and E5M1 shows that all models are in good agreement with Odin/SMR and ILAS/ILAS-II. Differences are generally in the range of ±20%. Larger differences (up to −40%) are found in all models at 500±25 K for N_2O mixing ratios greater than 200 ppb. Generally, the largest differences were found for the tropics and the lowest for the polar regions. However, an underestimation of polar winter ozone loss was found both in KASIMA and E5M1 both in the Northern and Southern Hemisphere.

ACPD

9, 1977–2020, 2009

1 Introduction

The slowly decreasing level of halogens in the stratosphere in the coming decades is expected to lead to a gradual recovery from the chemical ozone depletion that is clearly noticeable in the extratropics since ~1980 (WMO, 2007). However, in the future the stratosphere will be influenced through a range of processes (radiative, dynamical and chemical) resulting from increases in green-house gas concentrations and future IPCC reports will be based on climate models that include full representation of the stratosphere (Shaw and Shepherd, 2008). Therefore, an improved understanding of these processes as well as the interaction between chemistry and climate is needed if credible predictions of future levels of stratospheric ozone and its impact on climate and surface UV radiation are to be made (WMO, 2007; Eyring et al., 2006, 2007). A number of Chemistry-Climate Models (CCMs) have been developed in the recent decade in order to provide such predictions. Although a lot of progress has been made the prediction of current CCMs produce still a wide range of results concerning the timing and extent of the ozone layer recovery (WMO, 2007). Recent analyses of chemical ozone loss in the polar regions show a substantial underestimation of ozone loss in the Antarctic and a severe underestimation of ozone loss in the Arctic (Tilmes et al., 2007; Lemmen et al., 2006). Therefore, evaluating these models with measurements is essential.

Here, we use a method based on ozone (O_3) and nitrous oxide (N_2O) measurements to evaluate Chemical Transport Models (CTMs) as well as Chemistry Climate Models (CCMs). This method has been first presented by Proffitt et al. (2003) for the Northern Hemisphere lower stratosphere based on aircraft and balloon-borne measurements and has then been extended to the upper stratosphere and Southern Hemisphere by Khosrawi et al. (2004, 2006) using satellite data from the Improved Limb Atmospheric Spectrometers (ILAS and ILAS-II). However, the ILAS/ILAS-II data are restricted to the polar regions. In a follow-up study by Khosrawi et al. (2008) satellite data from the Odin/Sub Millimetre Radiometer (Odin/SMR) were used which allowed an extension

of the method to the entire Northern and Southern Hemisphere as well as a separation into polar, midlatitude and tropical regimes. A comparison of the ILAS/ILAS-II and Odin/SMR data sets in the polar regions showed that both data sets can be used for the evaluation of CTMs and CCMs. Thus, in Khosrawi et al. (2008) we could verify the ILAS/ILAS-II 1-year data set and demonstrate that limited sampling of a solar occultation instrument such as ILAS/ILAS-II does not constitute a problem in deriving such a data set of monthly averages of N_2O and O_3.

Here, we use 1-year data sets derived from Odin/SMR and ILAS/ILAS-II to evaluate simulations in the lower stratosphere of two CTMs, namely the Chemical Lagrangian Model of the Stratosphere (CLaMS) and the Karlsruhe Simulation Model of the Middle Atmosphere (KASIMA) as well as one CCM, the atmospheric chemistry general circulation model ECHAM5/MESSy1 (E5M1).

2 Model data

2.1 CLaMS

The Chemical Lagrangian Model of the Stratosphere (CLaMS) is a chemistry transport model which simulates the dynamics and chemistry of multiple air parcels along their trajectories (McKenna et al., 2002a,b; Konopka et al., 2004). The trajectories are determined from wind fields taken from European Centre for Medium-range Weather Forecasts (ECMWF) analyses. The mixing of air parcels, that is the interaction between neighboring air parcels, is introduced both by combining air parcels and adding new air parcels where the mixing intensity is driven by the deformation of the wind field (McKenna et al., 2002a). As the air parcels are distributed irregularly in space, the horizontal resolution is defined by the mean distance of neighboring air parcels on an isentropic surface. Vertical motion is calculated as the time derivative of potential temperature using the radiation scheme by Morcrette (1991). Here, we used a CLaMS simulation for the Northern Hemisphere with a horizontal resolution of 100 km

north 40° N and of 300 km between 40° N and the Equator (Grooß et al., 2005). As vertical coordinate potential temperature is used, divided into 30 equally spaced levels between 350 and 900 K. The CLaMS simulation used here started on 17 November 2002 and was run until 23 March 2003. The initialization of O_3 was based on the MIPAS/ENVISAT data from 16 and 17 November 2002. A detailed description of the CLaMS model and this simulation can be found in McKenna et al. (2002a,b) and Grooß et al. (2005).

2.2 KASIMA

The Karlsruhe Simulation Model of the Middle Atmosphere (KASIMA) is a mechanistical circulation model including stratospheric chemistry for the simulation of the behavior of physical and chemical processes in the middle atmosphere (Ruhnke et al., 1999; Reddmann et al., 2001). The meteorological component is based on a spectral architecture with the pressure altitude $z = -H \cdot \ln(p/p_0)$ as vertical coordinate where H=7 km is a constant atmospheric scale height, p is the pressure, and $p_0 = 1013.25$ hPa is a constant reference pressure. A horizontal resolution of T42 (2.8°×2.8°) has been used. In the vertical regime, 63 levels between 10 and 120 km pressure altitude and a 0.75 km spacing from 10 up to 22 km with an exponential increase above were used. The meteorology module of the KASIMA model consists of three versions: the diagnostic model, the prognostic model and the nudged model which combines the prognostic and diagnostic model (Kouker et al., 1999). In this study, the model is nudged towards the operational ECMWF analyses of temperature, vorticity and divergence between 7 and 48 km pressure altitude. Above 48 km pressure altitude the prognostic model has been used. The rate constants of the gas phase and heterogeneous reactions were taken from Sander et al. (2003). The photolysis rates are calculated online with the Fast-J2 scheme of Bian and Prather (2002). The distributions of chemical species in the KASIMA simulation used here were initialized on 30 March 2002 with results from a long-term KASIMA simulation.

2.3 ECHAM5/MESSy1

The atmospheric chemistry general circulation model ECHAM5/MESSy1 Version 1.4 (hereafter denoted as E5M1) is a combination of the general circulation model ECHAM5 (Roeckner et al., 2006) and the Modular Earth Submodel System (MESSy1, Jöckel et al., 2005, http://www.messy-interface.org). Here we analyse data for the year 2003 from the S1 simulation (covering the period 1998 to 2005) described by Jöckel et al. (2006). For this simulation a comprehensive atmospheric chemistry setup for the troposphere, the stratosphere and the lower mesosphere has been applied. The model simulation was performed in T42L90MA resolution, i.e., with a triangular truncation at wave number 42 for the spectral core of ECHAM5, which corresponds to a quadratic Gaussian grid of approximately 2.8°×2.8° degrees in latitude and longitude, and with 90 vertical layers from the surface up to 0.01 hPa (approx. 80 km). A Newtonian relaxation technique of the prognostic variables temperature, vorticity, divergence and the (logarithm of the) surface pressure above the boundary layer and below 100 hPa towards ECMWF operational analysis data has been applied, in order to nudge the model dynamics towards the observed meteorology. For further details of the model and the model setup of the S1 simulation, we refer to Jöckel et al. (2006).

In addition, we performed an E5M1 sensitivity simulation with the same horizontal, but a lower vertical resolution with 39 layers up to 0.01 hPa (T42L39MA). The chemistry setup was reduced to focus on stratospheric ozone chemistry with a simplified description of the tropospheric ozone chemistry. The MESSy-submodels used for this simulation describe the following processes: ONLEM for "online" emissions of tracers and aerosols, OFFLEM for "offline" emissions of tracers and aerosols, TNUDGE for tracer nudging (Kerkweg et al., 2006a), DRYDEP for dry deposition of trace gases and aerosols, SEDI for the sedimentation of aerosol particles (Kerkweg et al., 2006b), MECCA for the gas-phase chemistry (Sander et al., 2005), JVAL for the calculation of photolysis rates (Landgraf and Crutzen, 1998), SCAV for the scavenging and liquid phase chemistry in cloud and precipitation (Tost et al., 2006a), CONVECT for the pa-

rameterization of convection (Tost et al., 2006b), LNOX for the source of NO_x produced by lightning (Tost et al., 2007a), PSC for the processes related to polar stratospheric clouds (Buchholz, 2005), QBO for nudging the quasi-biennial oscillation (Giorgetta et al., 2006), PTRAC for additional prognostic tracers (Jöckel et al., 2008), CVTRANS for convective tracer transport, TROPOP for diagnosing the tropopause and boundary layer height, H_2O for stratospheric water vapor, RAD4ALL for the radiation calculation, HETCHEM for calculating reaction coefficients of heterogeneous reactions on aerosols (see Jöckel et al., 2006 and references therein) as well as CLOUD for calculating the cloud cover as well as cloud micro-physics including precipitation (Tost et al., 2007b). For this sensitivity simulation, covering the period from the begin of 2000 to the end of 2007, the model dynamics was also nudged (up to 10 hPa) towards the ECMWF operational analysis. For the analysis presented here, we used data for the year 2003.

3 Satellite data

3.1 Odin/SMR

The Odin satellite is operated by the Swedish Space Cooperation in cooperation with groups from France, Canada and Finland (Murtagh et al., 2002). Odin was launched on 20 February 2001 and carries two instruments, the Optical Spectrograph and Infrared Imaging System (OSIRIS) (Llewellyn et al., 2004) and the Sub-Millimetre Radiometer (SMR) (Frisk et al., 2003). Observations of thermal emission of trace gases originating from the Earth's limb are performed in a time-sharing mode with astronomical observations. In aeronomy mode, various target bands are dedicated to profile measurements of trace constituents relevant to stratospheric and mesospheric chemistry and dynamics such as O_3, ClO, N_2O, HNO_3, H_2O, CO, and NO, as well as isotopes of H_2O and O_3 (e.g., Murtagh et al., 2002). Aeronomy mode measurements are performed twice a week until April 2007 and every other day thereafter. A typical stratospheric mode scan covers the altitude range from 7 to 70 km with a resolution of ≈1.5 km in terms of

tangent altitude below 50 km and ≈5.5 km above. Usually, the latitude range between 82.5° S and 82.5° N is covered by the measurements (Urban et al., 2005a,b).

For the retrieval of vertical profiles from the spectral measurements of a limb scan (aeronomy level-2 processing) two similar data processors have been developed. Here, we use Odin/SMR version 2.1 (Chalmers v2.1) data from the 501.8 GHz band. N_2O and O_3 profiles are retrieved from ≈12 to 60 km and ≈13 to 65 km, respectively, with an altitude resolution of 1.5 km and 3 km, respectively. The Odin/SMR N_2O data are validated in the range ≈15–50 km. The systematic error is estimated to be ≤12 ppbv above 20 km and in the range of 12–35 ppbv (up to 10–15%) below (Urban et al., 2005a). Extensive validation of Odin/SMR has been conducted, especially with the space-borne sensors Michelson Interferometer for Passive Atmospheric Soundings (MIPAS), ACE-Fourier Transform Spectrometer (ACE-FTS) and the Aura Microwave Limb Sounder (Aura-MLS). Validation of Odin/SMR N_2O with MIPAS showed a good overall agreement within 4–7 ppbv (Urban et al., 2005b, 2006). Further, validation studies by Strong et al. (2008) and Lambert et al. (2007) showed a very good agreement of Odin/SMR with ACE-FTS (better than −20%) and with Aura-MLS (better than 4–10%), respectively. The systematic error of Odin/SMR O_3 measurements is estimated to be lower than 0.6 ppmv. Odin/SMR measurements of O_3 derived with the Chalmers Version 2.1 retrieval algorithm were validated by Jégou et al. (2008) and showed a good agreement of Odin/SMR Version 2.1 data with ground-based (−0.15±0.3 ppmv), balloon-borne (−0.7±1 ppmv) and space-borne sensors (−0.3±0.2 ppmv). The intercomparison of Odin/SMR ozone measurements with MIPAS and balloon sonde data by Jones et al. (2007) showed an agreement within 10% between 17 and 55 km (a maximum deviation of 0.42 ppmv) and 5–10% between 25 and 35 km (less than 0.5 ppmv below 33 km). The validation study of ACE-FTS ozone measurements (Dupuy et al., 2008) showed a good agreement between ACE-FTS and Odin/SMR. The agreement between both instruments is better than +14% (0.5 ppmv) below 25 km. Between 25 and 40 km the percent differences where somewhat larger, ranging between 13–20%.

3.2 ILAS/ILAS-II

The Improved Limb Atmospheric Spectrometers ILAS and ILAS-II used the solar occultation technique which measures the absorption of stratospheric species in the infrared region of solar radiation (Yokota et al., 2002; Oshchepkov et al., 2005). The measurements were made in high latitude regions of the Northern and Southern Hemisphere covering the latitudes from 56° N to 70° N and from 63° S to 88° S (ILAS) and between 54° N to 71° N and 64° S and 88° S (ILAS-II). Measurements of vertical profiles of O_3, HNO_3, NO_2, N_2O, CH_4, H_2O, CFC-11, CFC-12, $ClONO_2$, and N_2O_5 were made 14 times per day in each hemisphere (Nakajima et al., 2006a,b) with a vertical resolution of 1 km. ILAS was launched onboard the Earth Observing Satellite (ADEOS) on 17 August 1996 and measured continuously from 30 October 1996 to 30 June 1997 (Sasano et al., 1999) while ILAS-II was launched on 14 December 2002 onboard ADEOS-II and measured continuously from 2 April 2003 to 24 October 2003 (Nakajima et al., 2006b).

Here, we use ILAS Version 6.1 (Nakajima et al., 2006a) and ILAS-II Version 2 data. Validation studies of ILAS Version 5.2 and ILAS-II Version 1.4 ozone data (Sugita et al., 2002, 2006) show a good agreement with correlative measurements between 11 and 64 km and between 11 and 40 km, respectively. The validation of ILAS Version 6.1 nitrous oxide data by Kanzawa et al. (2002) shows a good agreement between 10 and 40 km while ILAS-II Version 1.4 nitrous oxide data tend to be 10% lower in comparison to the Odin/SMR data and balloon-borne measurements (Ejiri et al., 2006). The latest Version 2 of ILAS-II has been improved compared to the former Version 1.4 by an improved transmittance correction in the Northern Hemisphere, by using HITRAN 2004 (Rothman et al., 2005) parameters instead of HITRAN 2000 (Rothman et al., 2003) parameters and by an improved tangent height registration (Tanaka et al., 2007). The intercomparison studies of Version 1.4 and Version 2 target species by Griesfeller et al. (2008) and Wetzel et al. (2008) show an improvement of the O_3 data in the Northern Hemisphere compared to the former Version 1.4 and a good agreement with mea-

surements from MIPAS and the balloon-borne MIPAS-B, respectively, between 16 and 31 km. Differences between the two retrieval versions were small for N_2O and a good agreement with MIPAS and MIPAS-B measurements was found as well between 16 and 31 km.

4 The O_3/N_2O distribution in the polar lower stratosphere

Proffitt et al. (2003) have a suggested a somewhat different way to use stratospheric tracer-tracer correlations than in the commonly employed method to deduce chemical polar ozone loss (e.g., Proffitt et al., 1993; Tilmes et al., 2003; Müller et al., 2005). Proffitt et al. (2003) calculated monthly averages of N_2O and O_3 by binning the data by altitude or potential temperature and then averaging over a fixed interval of N_2O (20 ppbv). This method helps to separate O_3 variability due to latitudinal transport from photochemical changes. Thus, the changes in the families of curves derived by using the method of Proffitt et al. (2003) are not only caused by chemical ozone loss or production, but also by transport processes (Proffitt et al., 2003; Khosrawi et al., 2004, 2006, 2008). How diabatic descent influences the families of curves has been shown in detail by Khosrawi et al. (2008) using the relationship between N_2O and potential temperature. Here, we will only discuss how the families of curves are influenced by diabatic descent as well as by winter and summer ozone destruction in the Northern Hemisphere polar regions on the basis of a schematic figure (Fig. 1).

The general characteristic of the families of curves derived from monthly averages of N_2O and O_3 binned by altitude or potential temperature is a positive correlation (increasing N_2O with increasing O_3) at the upper levels (above 500 K or 20 km) and a negative correlation (decreasing N_2O with increasing O_3) at the lower levels (below 500 K). The positive correlation at the levels above 500 K is caused by diabatic descent of air from above the O_3 maximum (Proffitt et al., 2003). Strong descent results in a steepening of the positively correlated curves and thus, the stronger the descent the stronger the steepening (Khosrawi et al., 2004). How descent affects the curves in the

polar regions is schematically shown on one curve (25 km, ≈550 K) in Fig. 1 (bottom: left) for the Northern Hemisphere for June and November. In June when descent is weak a negative correlation is found while in November when descent increases in strength the correlation changes to positive (increasing N_2O with increasing O_3). Substantial subsidence is generally observed in the Northern and Southern Hemisphere polar regions from fall to spring (e.g., Proffitt et al., 1989; Tuck, 1989; Russell et al., 1993; Rosenfield et al., 1994).

Polar winter ozone loss causes an inflection of the curves and therefore a change of slope (Fig. 1, top: left). Thus, the slope of the curves change from negative (at high N_2O mixing ratios) to positive correlated (at low N_2O mixing ratios). In general, when the maximum ozone loss is reached, this change of slope develops into a minimum in O_3 at around 50 ppbv N_2O (especially in the Southern Hemisphere). Figure 1 (top: left) shows this schematically for the curve at 20 km altitude (≈500 K) comparing the months January and March for the Northern Hemisphere. In January a change of slope is already visible at 150 ppmv N_2O. In March this inflection has shifted to somewhat higher N_2O mixing ratio (200 pbbv) and O_3 mixing ratios have decreased for low N_2O mixing ratios due to photochemical ozone destruction (Fig. 1, top: left). Evidence for chlorine-catalyzed photochemical O_3 destruction during late winter and early spring was reported for both hemispheres for several winters in previous studies based on model results and observations (e.g., Müller et al., 1997; Manney et al., 2003; Tilmes et al., 2004; Goutail et al., 2005; WMO, 2007).

The polar summer ozone destruction tends to reduce the ozone mixing ratios and thus the magnitude of the negative O_3/N_2O slope above 25 km (≈550 K) as shown schematically in Fig. 1 (top: right) for the curves at 25 km (June and August). In August O_3 mixing ratios are lower for all corresponding N_2O mixing ratios than in June due to photochemical O_3 destruction. Summer ozone loss from NO_x catalysis is found in the Northern Hemisphere from May to August between ≈10 and 100 hPa in the high latitudes and midlatitudes (e.g., Farman et al., 1985; Brühl and Crutzen, 2000). A detailed description of the method and characteristics of the N_2O/O_3 distribution can

be found in Khosrawi et al. (2008) and references therein.

Reference curves can be derived from measured correlations of N_2O and O_3. Such reference curves have been e.g. derived from shuttle data and have a clear dependence on latitude (Michelsen et al., 1998). The reference curves for May midlatitudes (ATMOS Shuttle 1985), April high latitudes (ATMOS Shuttle 1993) and November tropics (ATMOS Shuttle 1994) are shown in Fig. 1 (bottom: right). These reference curves help to distinguish between the different air masses. In general, the tropical air has higher N_2O mixing ratios than the reference curve for the midlatitudes and the tropics while the midlatitude air is centered around the midlatitude reference curve and the high latitude air has N_2O mixing ratios that are lower than the high latitude and midlatitude reference curves. These reference curves were used by Khosrawi et al. (2008) to distinguish between the air masses measured by Odin/SMR.

5 Model evaluation

Here, we evaluate simulations of stratospheric ozone by the models CLaMS, KASIMA and E5M1. For this purpose, monthly averages of N_2O and O_3 were calculated from the model results. For the evaluation of CLaMS, KASIMA and E5M1 the 500±25 K and 650±25 K potential temperature level were chosen. These levels were chosen since at 500±25 K polar winter ozone loss is pronounced and at 650±25 K descent is pronounced. The Odin/SMR data were taken as reference since from Odin/SMR global measurements are available. This allows us to evaluate the models not only for the entire hemisphere (considering all latitudes between 0°–90°), but also separated into the latitude regimes high latitudes (60°–90°), midlatitudes (30°–60°) and low latitudes (0°–30°). Further, to investigate on the differences caused by using different data sets as reference, we will evaluate CLaMS, KASIMA and E5M1 for the polar regions using ILAS/ILAS-II as reference (Sect. 5.3). Furthermore, we asses the effect of using a coarser spatial resolution in the model simulation by comparing the E5M1 T42L90 simulation with a T42L39 simulation. The differences *D* be-

tween Odin/SMR, ILAS/ILAS-II, CLaMS, KASIMA and E5M1 are calculated as follows: $D=[\mu\,(\text{Model})-\mu\,(\text{Odin})]/\mu\,(\text{Odin})*100$, where μ denotes the O_3 mixing ratio at a given N_2O mixing ratio of the Odin/SMR measurement and the model simulation, respectively. We refer to a good agreement in case of differences within ±20% and to a reasonable agreement for differences within ±40%.

The evaluation was performed for the Northern Hemisphere for the months November to February. These months have been chosen since the CLaMS simulation covers only the months from November to March. However, these months are particularly suitable to test the performance of the models during the Arctic winter, that is, during a period of significant chemical O_3 loss. To give an overview over the performance of the models for each month of the year, we calculated the averages of the differences for each month (which will be discussed in Sect. 5.5).

The strategy of this evaluation was to not consider a certain winter, but to perform a general evaluation. The data of the models and the measurements were primarily taken for the year 2003. However, since the CLaMS simulation was performed for the winter 2002/2003, the months November and December are for 2002. Further, since the months considered here were measured by ILAS (and not by ILAS-II) this data is for the years 1996 (November and December) and 1997 (January and February). However, the principal dynamical and chemical processes in each winter are the same and only the strength of these processes changes from year to year, thus small differences can occur from the usage of different years but these differences are clearly distinguishable from model deficiencies (Khosrawi et al., 2006, 2008).

The evaluation of CLaMS, KASIMA and E5M1 is shown in Fig. 2 for the entire Northern Hemisphere, and, separated into latitude regimes, in Figs. 3–5. The range of standard deviation of the monthly averaged O_3 derived from Odin/SMR are marked as a grey shaded area while standard deviations of the models are not included to keep the figures more concise. Standard deviations of the models are generally <5 ppbv for N_2O and <0.5 ppmv for O_3.

5.1 All latitude regimes (NH)

In Fig. 2, the evaluation for the Northern Hemisphere for the months November to February is shown. As described in Sect. 4, a positive to flat correlation is found at 650±25 K and a negative correlation at 500±25 K. In November CLaMS, KASIMA and E5M1 agree quite well with Odin/SMR. In the monthly averages, solely at N_2O mixing ratios larger than 230 ppb lower O_3 mixing ratios are derived from the model simulations than derived from Odin/SMR observations. Here, the differences in the averaged O_3 mixing ratios increase up to −40%. While the KASIMA and E5M1 curves for 500±25 K do not extend to N_2O mixing ratio as low as derived from Odin/SMR (70 ppbv N_2O) lower N_2O mixing ratios are found in the CLaMS simulation (30 ppbv N_2O). This indicates that in CLaMS a stronger descent is simulated than observed in November while in KASIMA and E5M1 the descent is simulated slightly less than observed at that time. At 650±25 K CLaMS and E5M1 agree quite well with Odin/SMR with differences in the averaged O_3 mixing ratios within +10% and +20%, respectively. Somewhat larger differences (generally in the range of ±20%) are found for KASIMA, especially at N_2O mixing ratios lower than 100 ppbv and larger than 250 ppbv. Similar results are found for December, but in all models at 500±25 K as well as at 650±25 K larger deviations from Odin/SMR are found at N_2O greater 250 ppb which can be attributed to influence of air of tropical character (air with higher mixing ratios than the tropical reference curve, see Fig. 1, bottom: right), thus, indicating differences of the model simulation in the tropical regions (Fig. 2, December). These differences will be discussed in more detail in Sect. 5.2.1. However, the ozone differences for the averaged N_2O mixing ratios range generally within ±20% for all models.

From January on, ozone loss is visible at 500±25 K by an inflection and a change of slope from positively to negatively correlated. In the Odin/SMR monthly averages as well as in CLaMS and KASIMA monthly averages this inflection is found at 190 ppbv while in E5M1 this inflection is shifted slightly and is found at 210 ppbv (Fig. 2, left, January). This shift in the inflection is caused by an underdetermination of ozone destruc-

tion during polar winter in E5M1. Further, while in CLaMS, KASIMA and Odin/SMR the O_3 mixing ratios tend to decrease with decreasing N_2O this is not found in E5M1. Here, the mixing ratios tend rather to increase confirming too that polar ozone loss in the model is underestimated. This will be discussed in more detail in Sect. 5.2.3.

In general, the monthly averages of N_2O and O_3 derived from CLaMS, KASIMA and E5M1 simulations are in good agreement with Odin/SMR measurements with differences in O_3 mixing ratios in the range of ±20% if the entire Northern Hemisphere (all latitudes) is considered. Differences at 500±25 K are somewhat larger than at 650±25 K, especially at N_2O mixing ratios greater than 200 ppb (500±25 K) and 250 ppb (650±25 K), respectively, larger differences are found. In all models, differences increase here up to −40%.

5.2 Separation into latitude regimes (NH)

In the following the evaluation will be performed separately for three latitude regions: high latitudes (60° to 90° N), midlatitudes (30° to 60° N) and low latitudes (0° to 30° N). The tropics are not truly isolated from the midlatitudes and these are not truly isolated from the high latitudes (e.g. Tuck et al., 1989; Proffitt et al., 1989; Tuck and Proffitt, 1997; Randel et al., 1993; Michelsen et al., 1998; Proffitt et al., 2003). Data taken well outside the tropics can be of tropical character (Randel et al., 1993). However, the separation of the N_2O/O_3 data set into the different latitude regimes reveals the rather different characteristics of these air masses (Khosrawi et al., 2008). Generally, in the N_2O/O_3 distribution the region with low N_2O and high O_3 mixing ratios can be attributed to air of polar character and the region with high N_2O and low O_3 mixing ratios can be attributed to air of tropical character while the intermediate region of N_2O and O_3 mixing ratios characterize midlatitude air (Sect. 4 and Fig. 1, bottom: right).

5.2.1 Tropics

The CLaMS simulation investigated here was focusing on ozone loss in the polar regions and thus was performed with a much lower spatial resolution between 0 and 40° N acting mainly as a boundary for the high and midlatitudes. Therefore, the CLaMS data set is not considered in the evaluation of the tropics. In the tropics, changes of the N_2O/O_3 distribution from season to season and between the hemispheres are small (Khosrawi et al., 2008). A flat to positive correlation is generally found above 700 K. The positive correlation is caused by the photochemical production of ozone in the tropics. At potential temperature levels below 550 K the correlation is influenced by midlatitude air (Khosrawi et al., 2008). For the tropics, a good agreement is found for KASIMA and E5M1 at 650±25 K while a reasonable agreement is found for 500±25 K. At 500±25 K in both models a steeper negative correlation is found which leads to higher O_3 mixing ratios at N_2O mixing ratios smaller than 250 ppbv and lower O_3 mixing ratios at N_2O mixing ratios larger than 250 ppbv (Fig. 3, left, all months). Therefore, differences in averaged O_3 mixing ratios change from +40% to −40% with increasing N_2O. At 650±25 K differences are not exceeding ±20% and averaged O_3 derived from KASIMA and E5M1 are generally higher than the ones derived from Odin/SMR (Fig. 3, right, all months). The large differences at 500 K are partly caused by the fact that in the tropical regions large gradients in O_3 occur and these are interpolated onto a certain potential temperature level from a rather coarse altitude resolution (3 km) of Odin/SMR (thus too coarse to resolve these gradients properly). However, this differences could also be to some part be caused by model deficiencies. The steeper correlation in the models could be caused by a too strong mixing of midlatitude air into the tropical regions. To understand this difference in detail further data sets have to be taken into account. However, this is beyond the scope of this study. The same applies to the unusually high N_2O values found in the Odin/SMR monthly averages at 650±25 K (N_2O>300 ppb). It has to be noted that the reported statistical uncertainty of single Odin/SMR data points on that level is of the order of the chosen N_2O bins size

($1\sigma \approx 25$ ppbv). This may led to an artificial extension of the correlation curves at their ends. This argument is supported by the fact that a rather low number of data points is present in the bins for N_2O>300 ppb compared to other bins. Therefore, we do not further discuss here the monthly averages of O_3 and N_2O derived from Odin/SMR and the differences to the simulations for these bins.

5.2.2 Midlatitudes

In the midlatitudes generally a good agreement between CLaMS, KASIMA and E5M1 with Odin/SMR observations is found (Fig. 4). In November and December the differences at 650±25 K lie generally around ±10% (with a tendency to +10%) and in January and February at around +20%, thus showing generally larger ozone mixing ratios than measured (Fig. 4, right). At 500±25 K the differences are generally larger than at 650±25 K and a stronger negative correlation is found for N_2O mixing ratios greater than 200 ppbv as was also found in the evaluation for the tropics. The differences lie generally around ±20% especially for midlatitude N_2O mixing ratios less than 200 ppbv (which can be attributed to air of midlatitude and polar origin, see reference curves shown in Fig. 1, bottom: right). Larger differences up to (−50%) are found between the models and Odin/SMR for N_2O mixing ratios greater than 200 ppbv. Here, differences are gradually increasing with increasing N_2O due to the steeper correlation of the curves between 200 and 300 ppbv N_2O. These air massses can be attributed to air of tropical character as can be seen from the evaluation of the model simulations in the tropics discussed in the previous section.

At 500±25 K a larger amount of air of polar origin (N_2O mixing ratios less than 110 ppbv) is found in the CLaMS simulation in November and December than observed by Odin/SMR (Fig. 4, left). A somewhat larger amount is also found in the KASIMA simulation in December while in E5M1 a generally lower amount is found (see next section for further details). In February large differences are found between all models and Odin/SMR at low N_2O mixing ratios (Fig. 4, February). However, these differences are most likely caused by the comparably low number of data points in the bins and a high

variability of the Odin/SMR measurements (mixture between inside and outside of the vortex air) which also leads to the somewhat unrealistic zigzag shape for N_2O mixing ratios between 50 and 150 ppbv.

5.2.3 Polar regions

Since the ILAS/ILAS-II data are available for the polar regions this data set has been included in the evaluation for the polar regions (Fig. 5). Again a good agreement between CLaMS, KASIMA and E5M1 is found for 650±25 K. The small O_3 minimum found in the Odin/SMR data at 200 ppbv N_2O (650±25 K) in January is most likely caused by a comparably low number of data points in the bins and a high variability of the Odin/SMR measurements. This minimum is neither found in the ILAS/ILAS-II data nor in the model simulations. At 650±25 K the difference lies in the range of ±20%. In CLaMS and E5M1 a larger amount of air of midlatitude and tropical character is found (visible as the extension of the curve to larger N_2O mixing ratios).

Generally, at 650±25 K the differences remain the same (in the range of ±20%) for all months considered here (Fig. 5, right). Solely, the differences between ILAS/ILAS-II and E5M1 are somewhat larger in November for N_2O<30 ppbv and N_2O>170 ppbv (Fig. 5, right). The ILAS/ILAS-II measurements at 650±25 K show somewhat lower ozone mixing ratios than observed by Odin/SMR in November and December. Most likely the cause for this lower ozone mixing ratios is the fact that ILAS/ILAS-II measures closer to the pole than Odin/SMR and thus more air from inside the vortex and less air of midlatitude character. At 500±25 K differences are somewhat larger but also in the range of ±20%. Larger differences reaching up to −40% are found for N_2O mixing ratios greater than 200 ppbv. The data points can be attributed to air of tropical character as described already in the previous two sections. However, differences are smaller here than in the midlatitudes and tropics due to the mixing of the different air masses and thus the dilution of the air of tropical character (Fig. 5, right).

Polar winter ozone loss is visible at 500±25 K from January on by an inflection of the curves and thus a change of slope to negatively correlated and an extension to lower

N_2O mixing ratios (Fig. 5, left, January). In the Odin/SMR data this inflection between ILAS/ILAS-II and Odin/SMR is found at 190 ppbv N_2O and ILAS/ILAS-II at 150 ppbv. This difference in the inflection is most probably caused by differences in ozone loss in the winters 1996/1997 and 2002/2003 (all months shown here are taken from ILAS measurements, thus from 1996/1997). In the CLaMS, and KASIMA simulation the inflection is found at the same location as Odin/SMR. In the E5M1 simulation the inflection is found at somewhat higher N_2O mixing ratios (210 ppb instead of 190 ppb N_2O) and the O_3 mixing ratios are not as low as measured by Odin/SMR. The O_3 mixing ratios in E5M1 are rather increasing towards February which indicates that polar winter ozone loss is underestimated. A slight underestimation of polar ozone loss is also found in the KASIMA simulation since the O_3 mixing ratios are not reaching as low values as CLaMS or Odin/SMR, but for the CLaMS simulation a good agreement is found. An underestimation of polar ozone loss has also been observed in other CCMs, e.g. in the CCM WACCM (Whole-Atmosphere Community Climate Model). Tilmes et al. (2007) showed that Arctic ozone loss in spring is severely underestimated by WACCM. While the understimation of ozone loss in KASIMA is most probably caused only by a underestimation of the chemistry, in E5M1 the underestimation of ozone loss is most probably caused by both an underestimation of the chemistry as well as descent since the typical low O_3 mixing ratios found at low N_2O mixing ratios (<50 ppbv), thus an extention of the curve to lower N_2O values, are not found in the E5M1 simulation. At 650±25 K differences in the averaged O_3 mixing ratios are generally within ±20%, thus a good agreement is found here. A rather reasonable agreement with differences up to −40% is found for N_2O mixing ratios greater than 250 ppbv. In both levels the N_2O/O_3 distribution remains almost unchanged in all data sets from January to February.

5.3 Assessment on different data sets used for a model evaluation

In the following we will repeat the evaluation for the polar regions using the ILAS/ILAS-II data set as the reference data set to assess how the results change if this data set is used instead of Odin/SMR. The general characteristics of the monthly averages derived

from CLaMS, KASIMA and E5M1 are in agreement with the monthly averages derived from ILAS/ILAS-II measurements (Fig. 6).

Generally the difference between the ILAS/ILAS-II data and the CLaMS, KASIMA and E5M1 results are similar to the differences derived using the Odin/SMR data set as a reference. However, somewhat larger differences are found for CLaMS, KASIMA and E5M1 in November in December at 500±25 K compared to the evaluation using Odin/SMR as the reference (Fig. 6 compared to Fig. 5, right). Further, somewhat larger differences are also found to all three models in January and February at 650±25 K and at 500±25 K since at this level lower O_3 mixing ratios were measured by ILAS/ILAS-II than by Odin/SMR. This is due to the fact that ILAS/ILAS-II measurements are focused on the polar regions and thus a less air from outside the vortex (air that contains larger amounts of ozone) was sampled. Further, due to the focus of ILAS/ILAS-II on the polar regions and the usage of solar occultation technique, the N_2O/O_3 curves derived from ILAS/ILAS-II extend over a smaller N_2O range than the curves derived from Odin/SMR (Fig. 6 compared to Fig. 5).

Furthermore, the large differences which were found in the evaluation of CLaMS, KASIMA and E5M1 with Odin/SMR at N_2O mixing ratios greater than 200 ppbv due to air of tropical character are not found here since such air masses are not measured by ILAS/ILAS-II (Fig. 6, left). Thus, it seems, that the models show a stronger influence of air of polar and midlatitude character in the tropical regions. However, as discussed before these differences are also caused partly by the large vertical gradients in O_3 in the tropics which cannot be resolved properly by the coarse vertical resolution of the Odin/SMR measurements (3 km).

Using the ILAS/ILAS-II data set as reference for the model evaluation shows slight deviations in the absolute differences compared to than Odin/SMR is used as reference. However, the main result, that CLaMS, KASIMA and E5M1 are in good agreement (±20%) with the observations is also supported by the evaluation using ILAS/ILAS-II data as reference. Thus, both data set are suitable for a model evaluation. Of course, the ILAS/ILAS-II data set can only be used for an evaluation study for the

polar regions. If the entire hemisphere or a separation into latitude regimes is anticipated one needs to use the Odin/SMR data sets. Further, there are also other satellite measurements which can be used for deriving monthly averages of N_2O and O_3 and thus can be used for an evaluation study as presented here. Furthermore, we also would recommend to take all available data sets derived from satellite measurements into account for a model evaluation study.

5.4 Assessment on different vertical resolutions used in model simulations

To asses the impact of different vertical resolutions of the model simulation we compare the E5M1 simulation in T42L90MA resolution used in the evaluation study described in the previous sections with an E5M1 simulation with a T42L39MA resolution (Fig. 7, NH, all latitudes). Generally, the shape of the curves are similar, however differences of the T42L39MA data to Odin/SMR are somewhat larger, especially at 500±25 K than for the high resolution simulation. At 500±25 K ozone mixing ratios are generally higher in the T42L39MA simulation than in the T42L90MA simulation (November and December entire curve, January and February N_2O values greater than 200 ppbv). That E5M1 underestimates the polar ozone destruction during winter is a general problem of the model, however, much better results are derived with the E5M1 simulation with a higher vertical resolution. In the T42L39MA simulation the slope change is found at 230 ppbv (500 K, January) while it is found at 210 ppbv in the T42L90MA simulation, which is almost in agreement with Odin/SMR where the slope change is found at 190 ppbv (Fig. 7, left, January).

At 500 K, differences in ozone mixing ratios between E5M1 and Odin/SMR increase with decreasing N_2O towards February. In February, at 70 ppbv N_2O 4.2 ppmv O_3 are derived from both E5M1 simulations instead of 2.7 ppmv as derived from Odin/SMR observations (a difference of 1.7 ppmv and thus up to 65% more ozone in both simulations).

Another important difference is that in the simulation with lower resolution some artifacts are occuring, namely at the curve at 650±25 K in December. There is a peak

in O_3 at N_2O mixing ratios between 230 ppbv and 280 ppbv. This peak most likely occurs because of the quasi-biennial oscillation (QBO) which is treated differently in both simulations. In the E5M1 T42L39MA simulation the QBO is nudged while in the E5M1 T42L90MA simulation the QBO develops freely.

5.5 Average differences

An average of the differences in O_3 mixing ratios between CLaMS, KASIMA and E5M1 and Odin/SMR has been calculated for each month to give an overview of the performance of the models for each month of the year. While the KASIMA and E5M1 simulation cover an entire year the simulation of CLaMS covers only the winter period (November to March) and only for the Northern Hemisphere. The calculation of the average difference has been performed for the separation into the three latitude regimes: high latitude (60°–90°), midlatitude (30°–60°) and low latitudes (0°–30°). Since the CLaMS simulation focused on the polar regions the average of the differences has not been calculated for the low latitudes. Further, since ILAS/ILAS-II measurements only cover the polar regions the average of the differences of ILAS/ILAS-II have been calculated for the polar regions.

5.5.1 Northern Hemisphere

A good agreement between both satellite instruments, Odin/SMR and ILAS/ILAS-II, is found at 500±25 K (Fig. 8, solid lines). Differences in O_3 mixing ratios are lower than ±20%. At 650±25 K differences are about the same, but increase to 35% for the summer months (May to September). Thus, for the summer months only a reasonable agreement between ILAS/ILAS-II and Odin/SMR is found. Differences in O_3 mixing ratios between the models and Odin/SMR are generally within ±20%, but reach at some occasions up to 40% especially in the polar regions during summer months. Differences exceeding 20% are found in the polar regions at 500±25 K from February to September (KASIMA, up to 40%) and in April (E5M1, 25%) as well as at 650±25 K in May and August (E5M1, 25 and 30%). In the tropical regions, differences exceed-

ing 20% are found from April to October (KASIMA, up to 30%) and from February to September (E5M1, up to 25%). From the CLaMS simulation the summer months are not available since the simulation covers only the winter months, thus, we do not know whether differences higher than 20% are also found in CLaMS (Fig. 8, bottom). Nevertheless, the best agreement between CLaMS, KASIMA and E5M1 is found for the midlatitude region where differences between the models and Odin/SMR over the entire year are lower than ±20% (Fig. 8, middle).

5.5.2 Southern Hemisphere

Differences in the Southern Hemisphere are similar to the differences in the Northern Hemisphere (Fig. 9). For the polar regions, a good agreement is found between ILAS/ILAS-II and Odin/SMR at 500±25 K for all months except for October where differences increase up to −40% (Southern Hemisphere spring). This difference is caused by the fact that ILAS/ILAS-II measured at that time of the year very close to the pole and thus mainly air from inside the polar vortex where at that time low O_3 mixing ratios prevail because of chemical O_3 loss. At 650±25 K a good agreement is found between ILAS/ILAS-II and Odin/SMR (differences within ±20%) for all months except January where the difference reaches +40% (Fig. 9, top). As for the Northern Hemisphere the best agreement between the models and Odin/SMR is found for the midlatitudes with differences less than +20%. Solely, in the E5M1 simulation at 500±25 K differences up to −20% are reached in October and November (Fig. 9, middle panel). This "peak" in the E5M1 simulation is also found in the polar regions and can be attributed to an underestimation of chemical ozone destruction in the ozone hole region. Thus, in the E5M1 O_3 mixing ratios as low as measured under ozone hole conditions are not reached (Fig. 9, top). In E5M1 (not shown) the minimum O_3 values (1 ppmv) measured by Odin/SMR are reached, however, only for higher N_2O mixing ratios (50–110 ppbv) than in the Odin/SMR observations (10–120 ppbv). This will result in an underestimation of column O_3 loss in the ozone hole. Underestimation of chemical ozone loss in the Southern Hemisphere polar regions were recently also reported for the models

WACCM (Tilmes et al., 2007) and E39/C (Lemmen et al., 2006).

In the polar regions the differences between Odin/SMR and KASIMA as well as E5M1 lie generally between −10% and +30% (Fig. 9, top). Solely, differences up to −20% are found for the E5M1 simulation at 500±25 K in October as discussed above and up to 30% in September at 650±25 K. In the tropics the differences of KASIMA and E5M1 show the same shape with somehat larger differences in the KASIMA simulation at 500±25 K. However, differences lie generally within ±25% but increase gradually from −20% to +20% in July and decrease to −20% by December (Fig. 9, bottom).

6 Conclusions

Based on data sets of monthly averages of N_2O and O_3 derived from Odin/SMR and ILAS/ILAS-II we evaluated the CTMs CLaMS and KASIMA as well as the CCM E5M1 by using the method of (Proffitt et al., 2003). Using data from Odin/SMR allows to perform the evaluation for the entire hemisphere as well as separated into the latitude regions high, mid and low latitudes. Using additionally the ILAS/ILAS-II data set as the reference for the polar latitudes it could be shown that this data set is also adequate for a model evaluation, although it is, restricted to the polar latitudes since from ILAS/ILAS-II only measurements for this region are available.

In general, the data sets derived from the model simulations were in good agreement with the data set derived from Odin/SMR. Differences of the averaged O_3 mixing ratios derived from CLaMS, KASIMA and E5M1 from Odin/SMR were calculated. These differences were generally in the range of ±20% considering the entire hemisphere (0–90°). Larger differences up to ±40% (thus a reasonable agreement) were found at N_2O mixing ratios greater than 250 ppbv (tropical air and air of tropical character). A clear underestimation of ozone loss in polar winter is visible at 500±25 K in the KASIMA and E5M1 simulations. The underestimation of ozone loss in KASIMA is most likely caused by an underestimation of chemical winter ozone loss while in E5M1 most likely also descent in winter and early spring is underestimated since the typical low O_3 mixing ratios at low N_2O mixing ratios seen in the averages of Odin/SMR and ILAS/ILAS-II

were not simulated. The underestimation of ozone loss in E5M1 is a general model difficiency, however, the model results can be improved significantly if a higher vertical resolution is used as we showed comparing the E5M1 T42L39MA simulation with the T42L90MA simulation. Recent analyses of chemical ozone loss in the polar regions show that also other chemistry climate models signicantly underestimate ozone loss (Tilmes et al., 2007; Lemmen et al., 2006).

For the evaluation separated into latitude regimes (Figs. 3–5) the best agreement between models and Odin/SMR was found for the midlatitude regions and the largest differences for the tropics, but only at the 500±25 K level. This difference between models and Odin/SMR is partly caused by the large vertical O_3 gradients occurring in the tropical regions which cannot entirely be resolved by the rather coarse vertical resolution of Odin/SMR of 3 km, but probably also to some part by an overestimation of transport of polar and midlatitude air towards the tropical regions. To understand this difference between the models and Odin/SMR in detail further data sets have to be taken into account which was however beyond the scope of this study.

Considering averages of the differences of O_3 mixing ratios for each month over an entire year, ILAS/ILAS-II and Odin/SMR were generally in good agreement and differences were within ±20%. However, differences reaching up to ±40% where found in the Northern Hemisphere during summer and in the Southern Hemisphere during winter. Comparing these averaged differences of O_3 mixing ratios derived from the model simulations with Odin/SMR the best agreement was found in both hemispheres for the midlatitudes. Differences were generally within ±20% for both hemispheres and all latitude regimes. Larger differences were found occasionally in both hemispheres for the summer months in the tropics and polar regions. Thereby, differences reached up to 40% (KASIMA) at 500 K (NH) and up to 40% (E5M1) at 650 K (SH) in the polar regions. In the tropics the differences in the summer months reached up to 30% (KASIMA and E5M1) at 500 and 650 K (NH and SH). Since the CLaMS simulation was only performed for the winter months no evaluation of the summer months could be performed here. Nevertheless, the method presented here presents a promising tool for the evaluation

of atmospheric chemical models like CTMs and CCMs and was successfully applied to evaluate CLaMS, KASIMA and E5M1.

Acknowledgements. We are grateful to the European Space Agency (ESA) for providing the Odin/SMR data. Odin is a Swedish led project funded jointly by Sweden (SNSB), Canada (CSA), Finland (TEKES), and France (CNES) and the European Space Agency (ESA). The Improved Limb Atmospheric Spectrometer (ILAS and ILAS-II) were were developed by the Japanese Ministry of Environment (MOE) and were operated by the Japan Aerospace Exploration Agency (JAXA). The ILAS/ILAS-II data was processed at the ILAS and ILAS-II Data Handling Facility, National Institute of Environmental Studies (NIES), Japan. We would like to thank P. Achtert for helping with the graphic editing. We are also greatful to the Swedish Research Council for funding F. Khosrawi.

References

Bian, H. and Prather, M.: Fast-J2: Accurate simulation of stratospheric photolysis in global chemical models, J. Atmos. Chem., 41, 281–296, 2002. 1981

Brühl, C. and Crutzen, P. J.: NO_x-catalyzed ozone destruction and NO_x activation at midlatitudes to high latitudes as the main cause of the spring to fall stratospheric ozone decline in the Northern Hemisphere, J. Geophys. Res., 105, 12 163–12 168, 2000. 1987

Buchholz, J.: Simulations of physics and chemistry of polar stratospheric clouds with a general circulation model, Ph.D. thesis, Johannes Gutenberg University Mainz, 172 pp., 2005. 1983

Dupuy, E., Walker, K. A., Kar, J., Boone, C. D., McElroy, C. T., Bernath, P. F., Drummond, J. R., Skelton, R., McLeod, S. D., Hughes, R. C., Nowlan, C. R., Dufour, D. G., Zou, J., Nichitiu, F., Strong, K., Baron, P., Bevilacqua, R. M., Blumenstock, T., Bodeker, G. E., Borsdorff, T., Bourassa, A. E., Bovensmann, H., Boyd, I. S., Bracher, A., Brogniez, C., Burrows, J. P., Catoire, V., Ceccherini, S., Chabrillat, S., Christensen, T., Coffey, M. T., Cortesi, U., Davies, J., De Clercq, C., Degenstein, D. A., De Mazière, M., Demoulin, P., Dodion, J., Firanski, B., Fischer, H., Forbes, G., Froidevaux, L., Fussen, D., Gerard, P., Godin-Beekman, S., Goutail, F., Granville, J., Griffith, D., Haley, C. S., Hannigan, J. W., Höpfner, M., Jin, J. J., Jones, A., Jones, N. B., Jucks, K., Kagawa, A., Kasai, Y., Kerzenmacher, T. E., Kleinböhl, A., Klekociuk, A. R., Kramer, I., Küllmann, H., Kuttippurath, J., Kyrölä, E., Lambert, J.-C., Livesey, N. J., Llewellyn, E. J., Lloyd, N. D., Mahieu, E., Manney, G. L., Marshall, B. T., McConnell, J. C.,

McCormick, M. P., McDermid, I. S., McHugh, M., McLinden, C. A., Mellqvist, J., Mizutani, K., Murayama, Y., Murtagh, D. P., Oelhaf, H., Parrish, A., Petelina, S. V., Piccolo, C., Pommereau, J.-P., Randall, C. E., Robert, C., Roth, C., Schneider, M., Senten, C., Steck, T., Strandberg, A., Strawbridge, K. B., Sussmann, R., Swart, D. P. J., Tarasick, D. W., Taylor, J. R., Tétard, C., Thomason, L. W., Thompson, A. M., Tully, M. B., Urban, J., Vanhellemont, F., von Clarmann, T., von der Gathen, P., von Savigny, C., Waters, J. W., Witte, J. C., Wolff, M., and Zawodny, J. M.: Validation of ozone measurements from the Atmospheric Chemistry Experiment (ACE), Atmos. Chem. Phys. Discuss., 8, 2513–2656, 2008, http://www.atmos-chem-phys-discuss.net/8/2513/2008/. 1984

Ejiri, M. K., Terao, Y., Sugita, T., Nakajima, H., Yokota, T., Toon, G. C., Sen, B., Wetzel, G., Oelhaf, H., Urban, J., Murtagh, D., Irie, H., Saitoh, N., Tanaka, T., Kanzawa, H., Shiotani, M., Kobayashi, H., and Sasano, Y.: Validation of ILAS-II V1.4 nitrous oxide and methane profiles, J. Geophys. Res., 111, D22S90, doi:10.1029/2005JD006449, 2006. 1985

Eyring, V., Butchart, N., Waugh, D. W., Akiyoshi, H., Austin, J., Bekki, S., Bodeker, G. E., Boville, B. A., Brühl, C., Chipperfield, M. P., Cordero, E., Dameris, M., Deushi, M., Fioletov, V. E., Frith, S. M., Garcia, R. R., Gettelman, A., Giorgetta, M. A., Grewe, V., Jourdain, L., Kinnison, D. E., Mancini, E., Manzini, E., Marchand, M., Marsh, D. R., Nagashima, T., Nielsen, E., Newman, P. A., Pawson, S., Pitari, G., Plummer, D. A., Rozanov, E., Schraner, M., Shepherd, T. G., Shibata, K., Stolarski, R. S., Struthers, H., Tian, W., and Yoshiki, M.: Assessment of temperature, trace species and ozone in chemistry-climate simulations of the recent past, J. Geophys. Res., 111, D22 308,10.1029/2006JD007327, 2006. 1979

Eyring, V., Waugh, D. W., Bodeker, G. E., Cordero, E., Akiyoshi, H., Austin, J., Beagley, S. R., Boville, B. A., Braesicke, P., Brühl, C., Butchart, N., Chipperfield, M. P., Dameris, M., Deckert, R., Deushi, M., Frith, S. M., Garcia, R. R., Gettelmann, A., Giorgetta, M. A., Kinneson, D. E., Mancini, E., Manzini, E., Marsh, D. R., Matthes, S., Nagashima, T., Newman, P. A., Nielson, J. E., Pawson, S., Pitari, G., Plummer, D. A., Rozanov, R., Schraner, M., Scinocca, J. F., Semeniuk, K., Shepherd, T. G., Shibata, K., Steil, B., Stolarski, R. S., Tian, W., and Yoshiki, M.: Multimodal projections of stratospheric ozone in the 21th century, J. Geophys. Res., 112, D16303, doi:10.1029/2006JD008332, 2007. 1979

Farman, J. C., Murgatroyd, R. J., Silnickas, A. M., and Thrush, B. A.: Ozone photochemistry in the Antarctic stratosphere in summer, Q. J. Roy. Meteor. Soc., 111, 1013–1025, 1985. 1987

Frisk, U., Gastrom, M., Ala-Laurinaho, J., Andersson, S., Berges, J. C., Chabaud, J. P., Dahlgren, M., Emrich, A., Florin, G. F., Fredrixon, M., et al.: The Odin satellite: I. Radiometer

design and test, Astron. Astrophys., 403, 27–34, 2003. 1983
Giorgetta, M. A., Manzini, E., Roeckner, E., Esch, M., and Bengtsson, L.: Climatology and forcing of the quasi-biennial oscillation in the MAECHAM5 model, J. Climate, 19, 3882–3901, 2006. 1983
Goutail, F., Pommereau, J.-P., Lefèvre, F., van Roozendael, M., Andersen, S. B., Kåstad Hiskar, B.-A., Dorokhov, V., Kyrö, E., Chipperfield, M. P., and Feng, W.: Early unusual ozone loss during the Arctic winter 2002/2003 compared to other winters, Atmos. Chem. Phys., 5, 665–677, 2005, http://www.atmos-chem-phys.net/5/665/2005/. 1987
Griesfeller, A., von Clarmann, T., Griesfeller, J., Höpfner, M., Milz, M., Nakajima, H., Steck, T., Sugita, T., Tanaka, T., and Yokota, T.: Intercomparison of ILAS-II version 1.4 and version 2 target parameters with MIPAS-Envisat measurements, Atmos. Chem. Phys., 8, 825–843, 2008, http://www.atmos-chem-phys.net/8/825/2008/. 1985
Grooß, J.-U., Günther, G., Müller, R., Konopka, P., Bausch, S., Schlager, H., Voigt, C., Volk, C.M., and Toon, G. C.: Simulation of denitrification and ozone loss for the Arctic winter 2002/2003, Atmos. Chem. Phys., 5, 1437–1448, 2005, http://www.atmos-chem-phys.net/5/1437/2005/. 1981
Jégou, F., Urban, J., de La Noë, J., Ricaud, P., Le Flochmoën, E., Murtagh, D. P., Eriksson, P., Jones, A., Petelina, S., Llewellyn, E. J., Lloyd, N. D., Haley, C., Lumpe, J., Randall, C., Bevilacqua, R. M., Catoire, V., Huret, N., Berthet, G., Renard, J. B., Strong, K., Davies, J., Mc Elroy, C. T., Goutail, F., and Pommereau, J. P.: Technical Note: Validation of Odin/SMR limb observations of ozone, comparisons with OSIRIS, POAM III, ground-based and balloon-borne instruments, Atmos. Chem. Phys., 8, 3385–3409, 2008, http://www.atmos-chem-phys.net/8/3385/2008/. 1984
Jöckel, P., Sander, R., Kerkweg, A., Tost, H., and Lelieveld, J.: Technical Note: The Modular Earth Submodel System (MESSy) – a new approach towards Earth System Modeling, Atmos. Chem. Phys., 5, 433–444, 2005, http://www.atmos-chem-phys.net/5/433/2005/. 1982
Jöckel, P., Tost, H., Pozzer, A., Brühl, C., Buchholz, J., Ganzeveld, L., Hoor, P., Kerkweg, A., Lawrence, M. G., Sander, R., Steil, B., Stiller, G., Tanarhte, M., Taraborrelli, D., van Aardenne, J., and Lelieveld, J.: The atmospheric chemistry general circulation model ECHAM5/MESSy1: consistent simulation of ozone from the surface to the mesosphere, Atmos. Chem. Phys., 6, 5067–5104, 2006, http://www.atmos-chem-phys.net/6/5067/2006/. 1982, 1983
Jöckel, P., Kerkweg, A., Buchholz-Dietsch, J., Tost, H., Sander, R., and Pozzer, A.: Technical

Note: Coupling of chemical processes with the Modular Earth Submodel System (MESSy) submodel TRACER, Atmos. Chem. Phys., 8, 1677–1687, 2008, http://www.atmos-chem-phys.net/8/1677/2008/. 1983

Jones, A., Murtagh, D., Urban, J., Eriksson, P., and Rösevall, J.: Intercomparison of Odin/SMR ozone measurements with MIPAS and ballon sonde data, Can. J. Phys., 85(11), 1111–1123, 2007. 1984

Kanzawa, H., Schiller, C., Ovarlez, J., Camy-Peyret, C., Payan, S., Jeseck, P., Oelhaf, H., Stowasser, M., Traub, W. A., Jucks, K. W., Johnson, D. G., Toon, G. C., Sen, B., Blavier, J.-F., Park, J. H., Bodeker, G. E., Pan, L. L., Sugita, T., Nakajima, H., Yokota, T., Suzuki, M., Shiotani, M., and Sasano, Y.: Validation and data characteristics of water vapor profiles observed by the Improved Limb Atmospheric Spectrometer (ILAS) and processed with the version 5.20 algorithm, J. Geophys. Res., 107, 8217, doi:10.1029/2001JD000881, (Correction, J. Geophys. Res., 108(D4), 8218, doi:10.1029/20003JD001601, 2003), 2002. 1985

Kerkweg, A., Buchholz, J., Ganzeveld, L., Pozzer, A., Tost, H., and Jöckel, P.: Technical Note: An implementation of the dry removal processes DRY DEPosition and SEDImentation in the Modular Earth Submodel System (MESSy), Atmos. Chem. Phys., 6, 4617–4632, 2006a, http://www.atmos-chem-phys.net/6/4617/2006/. 1982

Kerkweg, A., Sander, R., Tost, H., and Jöckel, P.: Technical note: Implementation of prescribed (OFFLEM), calculated (ONLEM), and pseudo-emissions (TNUDGE) of chemical species in the Modular Earth Submodel System (MESSy), Atmos. Chem. Phys., 6, 3603–3609, 2006b, http://www.atmos-chem-phys.net/6/3603/2006/. 1982

Khosrawi, F., Müller, R., Proffitt, M. H., and Nakajima, H.: Monthly averaged ozone and nitrous oxide from the Improved Limb Atmospheric Spectrometer (ILAS) in the Northern and Southern Hemisphere polar regions, J. Geophys. Res., 109, D10301, doi:10.1029/2003JD004365, 2004. 1979, 1986

Khosrawi, F., Müller, R., Proffitt, M. H., and Nakajima, H.: Monthly averages of nitrous oxide and ozone for the northern and southern hemisphere high latitudes: A "1-year climatology" derived from ILAS/ILAS-II observations, J. Geophys. Res., 111, D11S11, doi:10.1029/2005JD006384, 2006. 1979, 1986, 1989

Khosrawi, F., Müller, R., Proffitt, M. H., Urban, J., Murtagh, D. P., Ruhnke, R., Grooß, J.-U., and Nakajima, H.: The seasonal cycle of averages of nitrous oxide and ozone in the Northern and Southern Hemisphere polar, midlatitude and tropical regions derived from ILAS/ILAS-II and Odin/SMR observations, J. Geophys. Res., 113, D18305, doi:10.1029/2007JD009556,

2008. 1979, 1980, 1986, 1988, 1989, 1991, 1992

Konopka, P., Steinhorst, H.-M., Grooß, J.-U., Günther, G., R., M., Elkins, J. W., Jost, H.-J., Richard, E., Schmidt, U., Toon, G., and McKenna, D. S.: Mixing and ozone loss in the 1999–2000 Arctic vortex: Simulations with the three-dimensional Chemical Lagrangian Model of the Stratosphere CLaMS, J. Geophys. Res., 109, D02315, doi:10.1029/2003JD003792, 2004. 1980

Kouker, W., Langbein, I., Reddmann, T., and Ruhnke, R.: The Karlsruhe Simulation Model of the Middle Atmosphere (KASIMA), Version 2, Wiss. Ber. No. 6278, Institut für Meteorologie und Klimaforschung, Forschungszentrum Karlsruhe, 60 pp., 1999. 1981

Lambert, A., Read, W. G., Livesey, N. J., Santee, M. L., Manney, G. L., Froidevaux, L., Wu, D. L., Schwartz, M. J., Pumphrey, H. C., Jimenez, C., Nedoluha, G. E., Cofield, R. E., Cuddy, D. T., Daffer, W. H., Drouin, B. J., Fuller, R. A., Jarnot, R. F., Knosp, B. W., Pickett, H. M., Perun, V. S., Snyder, W. V., Stek, P. C., Thurstans, R. P., Wagner, P. A., Waters, J. W., Jucks, K. W., Toon, G. C., Stachnik, R. A., Bernath, P. F., Boone, C. D., Walker, K. A., Urban, J., Murtagh, D., Elkins, J. W., and Atlas, E.: Validation of the Aura Microwave Limb Sounder middle atmosphere water vapor and nitrous oxide measurements, J. Geophys. Res., 112, D24S36, doi:10.1029/2007JD008724, 2007. 1984

Landgraf, J. and Crutzen, P. J.: An efficient method for online calculations of photolysis and heating rates, J. Atmos. Sci., 55, 863–878, 1998. 1982

Lemmen, C., Dameris, M., Müller, R., and Riese, M.: Chemical ozone loss in a chemistry-climate model from 1960 to 1999, Geophys. Res. Lett., 33, L15820, doi:10.1029/2006GL026939, 2006. 1979, 2000, 2001

Llewellyn, E. J., Lloyd, N. D., Degenstein, D. A., Gattinger, R. L., Petelina, S. V., Bourassa, A. E., Wiensz, J. T., Ivanov, E. V., Dade, I. C. M., Solhem, B. H., Connell, J. C. M., Haley, J. C., and von Savigny, C., et al.: The OSIRIS instrument on the Odin spacecraft, Can. J. Phys., 82, 411–422, 2004. 1983

Manney, G. L., Froidevaux, L., Santee, M. L., Livesey, N. J., Sabutis, J. L., and Waters, J. W.: Variability of ozone loss during Arctic winter (1991 to 2000) estimated from UARS Microwave Limb Sounder measurements, J. Geophys. Res., 108, 4149, doi:10.1029/2002JD002634, 2003. 1987

McKenna, D. S., Konopka, P., Grooß, J.-U., Günther, G., Müller, R., Spang, R., Offermann, D., and Orsolini, Y.: A new Chemical Lagrangian Model of the Stratosphere (CLaMS): 1. Formulation of advection and mixing, J. Geophys. Res., 107, 4309, doi:10.1029/2000JD000114,

2002a. 1980, 1981
McKenna, D. S., Grooß, J.-U., Günther, G., Konopka, P., Müller, R., Carver, G., and Sasano, Y.: A new Chemical Lagrangian Model of the Stratosphere (CLaMS): 2. Formulation of chemistry-scheme and initialisation, J. Geophys. Res., 107, 4265, doi:10.1029/2000JD000113, 2002b. 1980, 1981
Michelsen, H. A., Manney, G. L., Gunson, M. R., and Zander, R.: Correlations of stratospheric abundances of NO_y, O_3, N_2O, and CH_4 derived from ATMOS measurements, J. Geophys. Res., 103, 28 347–28 359, 1998. 1988, 1991
Morcrette, J.-J.: Radiation and cloud radiative properties in the European Centre for Medium Range Weather Forecasts forecasting system, J. Geophys. Res., 96, 9121–9132, 1991. 1980
Müller, R., Grooß, J.-U., McKenna, D., Crutzen, P. J., Brühl, C., Russell, J. M., and Tuck, A. F.: HALOE observations of the vertical structure of chemical ozone depletion in the Arctic vortex during winter and early spring 1996–1997, Geophys. Res. Lett., 24, 2717–2720, 1997. 1987
Müller, R., Tilmes, S., Konopka, P., Grooß, J.-U., and Jost, H.-J.: Impact of mixing and chemical change on ozone-tracer relations in the polar vortex, Atmos. Chem. Phys., 5, 3139–3151, 2005, http://www.atmos-chem-phys.net/5/3139/2005/. 1986
Murtagh, D., Frisk, U., Merino, F., Ridal, M., Jonsson, A., Stegman, J., Witt, G., Eriksson, P., Jimenez, C., et al.: An overview of the Odin atmospheric mission, Can. J. Phys., 80, 309–319, 2002. 1983
Nakajima, H., Sugita, T., Irie, H., Saitoh, N., Oelhaf, H., Wetzel, G., Toon, G. C., Sen, B., Traub, W. A., Jucks, K., Yokota, T., and Sasano, Y.: Measurements of $ClONO_2$ by the Improved Limb Atmospheric Spectrometer (ILAS) in high latitude stratosphere: New products of version 6.1 data processing, J. Geophys. Res., 111, D11S09, doi:10.1029/2005JD006441, 2006a. 1985
Nakajima, H., Sugita, T., Yokota, T., Kobayashi, H., Sasano, Y., Ishigaki, T., Mogi, Y., Araki, N., Waragai, N., Kumura, N., Iwasawa, T., Kuze, T., Tanii, J., Togami, T., Kawasaki, H., Horikawa, M., and Uemura, N.: Characteristics and performance of the Improved Limb Atmospheric Spectrometer-II (ILAS-II) on board the ADEOS-II satellite, J. Geophys. Res., 111, D11S01, doi:10.1029/2005JD006334, 2006b. 1985
Oshchepkov, S., Sasano, Y., Yokota, T., Uemura, N., Matsuda, H., Itou, Y., and Nakajima, H.: Simultaneous stratospheric gas and aerosol retrievals from broadband infrared occulation measurements, Appl. Optics, 22, 4775–4784, 2005. 1985
Proffitt, M. H., Kelly, K. K., Powell, J. A., Gary, B. L., Loewenstein, M., Podolske, J. R., Strahan, S. E., and Chan, K. R.: Evidence of diabatic cooling and poleward transport within and around the

1987 Antarctic Ozone Hole, J. Geophys. Res., 94, 16 797–16 813, 1989. 1987, 1991
Proffitt, M. H., Aikin, K., Margitan, J. J., Loewenstein, M., Podolske, J. R., Weaver, A., Chan, K. R., Fast, H., and Elkins, J. W.: Ozone loss inside the northern polar vortex during the 1991–1992 winter, Science, 261, 1150–1154, 1993. 1986
Proffitt, M. H., Aikin, K., Tuck, A. F., Margitan, J. J., Webster, C. R., Toon, G. C., and Elkins, J. W.: Seasonally averaged ozone and nitrous oxide in the Northern Hemisphere lower stratosphere, J. Geophys. Res., 108(D3), 4110, doi:10.1029/2002JD002657, 2003. 1979, 1986, 1991, 2000
Randel, W. J., Gille, J. C., Roche, A. E., Kumer, J. B., Mergenthaler, J. L., Waters, J. W., Fishbein, E. F., and Lahoz, W. A.: Stratospheric transport from the tropics to middle latitudes by planetary-wave mixing, Nature, 365, 533–535, 1993. 1991
Reddmann, T., Ruhnke, R., and Kouker, W.: Three-dimensional model simulations of SF_6 with mesospheric chemistry, J. Geophys. Res., 106, 14 525–14 537, 2001. 1981
Roeckner, E., Brokopf, R., Esch, M., Giorgetta, M., Hagemann, S., Koernblueh, L., Manzini, E., Schlese, U., and Schulzweida, U.: Sensitivity of simulated climate to horizontal and vertical resolution in the ECHAM5 atmosphere model, J. Climate, 19, 3771–3791, 2006. 1982
Rosenfield, J. E., Newman, P. A., and Schoeberl, M. R.: Computations of diabatic descent in the stratospheric polar vortex, J. Geophys. Res., 99, 16 677–16 689, 1994. 1987
Rothman, L. S., Barbe, A., Benner, D. C., Brown, L. R., Camy-Peyret, C., Carleer, M. R., Chance, K., Clerbaux, C., Dana, V., Devi, V. M., Fayt, A., Flaud, J.-M., Gamache, R. R., Goldman, A., Jaquemart, D., Jucks, K. W., Lafferty, W. J., Mandin, J.-Y., Massie, S. T., Nemtchinov, V., Newnham, D. A., Perrin, A., Rinsland, C. P., Schroeder, J., Smith, K. M., Smith, M. A. H., Tang, K., Roth, R. A., Auwera, J. V., Varanasi, P., and Yoshino, K.: The HITRAN molecular spectroscopic database: Edition of 2000 including updates through 2001, J. Quant. Spectrosc. Ra., 82, 5–44, 2003. 1985
Rothman, L. S., Jaquemart, D., Barbe, A., Benner, D. C., Birk, M., Brown, L. R., Carleer Jr., M. R., C. C., Chance, K., Coudert, L., Dana, V., Devi, V. M., Flaud, J.-M., Gamache, R. R., Goldman, A., Hartmann, J.-M., Jucks, K. W., Maki, A. G., Mandin, J.-Y., Massie, S. T., Orphal, J., Perrin, A., Rinsland, C. P., Smith, M. A. H., Tennyson, J., Tolchenov, R. N., Toth, R. A., Auwera, J. V., Varanasi, P., and Wagner, G.: The HITRAN 2004 molecular spectroscopic database, J. Quant. Spectrosc. Rad., 96, 139–204, 2005. 1985
Ruhnke, R., Kouker, W., and Reddmann, T." The influence of the $OH+NO_2+M$ reaction on the NO_y partitioning in the late Arctic winter 1992/1993 as studied with KASIMA, J. Geophys.

Res., 104, 3755–3772, 1999. 1981
Russell, J. M., Tuck, A. F., Gordley, L. L., Park, J. H., Drayson, S. R., Harries, J. E., Cicerone, R. J., and Crutzen, P. J.: HALOE Antarctic observations in spring 1991, Geophys. Res. Lett., 20, 719–722, 1993. 1987
Sander, R., Kerkweg, A., Jöckel, P., and Lelieveld, J.: Technical note: The new comprehensive atmospheric chemistry module MECCA, Atmos. Chem. Phys., 5, 445–450, 2005, http://www.atmos-chem-phys.net/5/445/2005/. 1982
Sander, S. P., Friedl, R. R., Ravishankara, A. R., Golden, D. M., Kolb, C. E., Kurylo, M. J., Huie, R. E., Orkin, V. L., Molina, M. J., Moortgat, G. K., and Finnlaysen-Pitts, B. J.: Chemical kinetics and photochemical data for the use in atmospheric studies, Evaluation Number 14, JPL Publication 02–25, 2003. 1981
Sasano, Y., Suzuki, M., Yokota, T., and Kanzawa, H.: Improved Limb Atmospheric Spectrometer (ILAS) for stratospheric ozone layer measurements by solar occultation technique, Geophys. Res. Lett., 26, 197–200, 1999. 1985
Shaw, T. and Shepherd, T. G.: Raising the roof, Nature Geopscience, 1, 12–13, 2008. 1979
Strong, K., Wolff, M. A., Kerzenmacher, T. E., Walker, K. A., Bernath, P. F., Blumenstock, T., Boone, C., Catoire, V., Coffey, M., De Mazière, M., Demoulin, P., Duchatelet, P., Dupuy, E., Hannigan, J., Höpfner, M., Glatthor, N., Griffith, D. W. T., Jin, J. J., Jones, N., Jucks, K., Kuellmann, H., Kuttippurath, J., Lambert, A., Mahieu, E., McConnell, J. C., Mellqvist, J., Mikuteit, S., Murtagh, D. P., Notholt, J., Piccolo, C., Raspollini, P., Ridolfi, M., Robert, C., Schneider, M., Schrems, O., Semeniuk, K., Senten, C., Stiller, G. P., Strandberg, A., Taylor, J., Tétard, C., Toohey, M., Urban, J., Warneke, T., and Wood, S.: Validation of ACE-FTS N_2O measurements, Atmos. Chem. Phys., 8, 4759–4786, 2008, http://www.atmos-chem-phys.net/8/4759/2008/. 1984
Sugita, T., Yokota, T., Nakajima, H., Kanzawa, H., Nakane, H., H.Gernandt, Yushkov, V., Shibasaki, K., Deshler, T., Kondo, Y., Godin, S., Goutail, F., Pommereau, J. P., Camy-Peret, C., Payan, S., Jeseck, P., Renard, J.-B., Bösch, H., Fitzenberger, R., Pfeilsticker, K., von König, M., Bremer, H., Küllmann, H., Schlager, H., Margitan, J. J., Stachnik, B., Toon, G. C., Jucks, K., Traub, W. A., Johnson, D. G., Murata, I., Fukunishi, H., and Sasano, Y.: Validation of ozone measurements from the Improved Limb Atmospheric Spectrometer (ILAS), J. Geophys. Res., 107, 8212, doi:10.1029/2001JD000602, 2002. 1985
Sugita, T., Nakajima, H., Yokota, T., Kanzawa, H., Gernandt, H., Herber, A., van den Gathen, P., Koenig-Langlo, G., Sato, K., Dorokhov, V., Yushukov, V. A., Murayama, Y., Ya-

mamori, M., Godin-Beekmann, S., et al.: A comparative study of ozone profiles in the stratosphere and the lower mesosphere measured by the Improved Limb Atmospheric Spectrometer (ILAS-II), ozonsondes, and satellite profiles, J. Geophys. Res., 111, D11S02, doi:10.1029/2005JD006439, 2006. 1985

Tanaka, T., Nakajima, H., Sugita, T., Ejiri, M. K., Irie, H., Saitoh, N., Terao, Y., Kawasaki, H., Usami, M., Kawasaki, H., Yokota, T., Kobayashi, H., and Sasano, Y.: Tangent height registration method for the Version 1.4 data retrieval algorithm of the solar occultation sensor ILAS-II, Appl. Optics, 46, 7196–7201, 2007. 1985

Tilmes, S., Müller, R., Grooß, J.-U., McKenna, D. S., Russell, J. M., and Sasano, Y.: Calculation of chemical ozone loss in the Arctic winter 1996–1997 using ozone-tracer correlations: Comparison of Improved Limb Atmospheric Spectrometer (ILAS) and Halogen Occultation (HALOE) results, J. Geophys. Res., 108, 4045, doi:10.1029/2002JD002213, 2003. 1986

Tilmes, S., Mller, R., Groo, J.-U., and Russell III, J. M.: Ozone loss and chlorine activation in the Arctic winters 1991–2003 derived with the tracer-tracer correlations, Atmos. Chem. Phys., 4, 2181–2213, 2004, http://www.atmos-chem-phys.net/4/2181/2004/. 1987

Tilmes, S., Kinnison, D., Müller, R., Sassi, F., Marsh, D. R., Boville, B. A., and Garcia, R.: Evaluation of heterogeneous processes in the polar lower stratosphere in WACCM3, J. Geophys. Res., 112, D24302, doi:10.1029/2006JD008334, 2007. 1979, 1995, 2000, 2001

Tost, H., Jöckel, P., Kerkweg, A., Sander, R., and Lelieveld, J.: Technical note: A new comprehensive SCAVenging submodel for global atmospheric chemistry modelling, Atmos. Chem. Phys., 6, 565–574, 2006a, http://www.atmos-chem-phys.net/6/565/2006/. 1982

Tost, H., Jöckel, P., and Lelieveld, J.: Influence of different convection parameterisations in a GCM, Atmos. Chem. Phys., 6, 5475–5493, 2006b, http://www.atmos-chem-phys.net/6/5475/2006/. 1983

Tost, H., Jöckel, P., and Lelieveld, J.: Lightning and convection parameterisations - uncertainties in global modelling, Atmos. Chem. Phys., 7, 4553–4568, 2007a, http://www.atmos-chem-phys.net/7/4553/2007/. 1983

Tost, H., Jöckel, P., Kerkweg, A., Pozzer, A., Sander, R., and Lelieveld, J.: Global cloud and precipitation chemistry and wet deposition: tropospheric model simulations with ECHAM5/MESSy1, Atmos. Chem. Phys., 7, 2733–2757, 2007b, http://www.atmos-chem-phys.net/7/2733/2007/. 1983

Tuck, A. F.: Synoptic and chemical evolution of the Antarctic vortex in late winter and early spring, 1987, J. Geophys. Res., 94, 11 687–11 737, 1989. 1987

Tuck, A. F. and Proffitt, M. H.: Comment on "On the magnitude of transport out of the Antarctic polar vortex" by Wiel M. F. Wauben et al., J. Geophys. Res., 102, 28 215–28 218, 1997. 1991

Tuck, A. F., Watson, R. T., Condon, E. P., and Toon, J. J. M. O. B.: The planning and execution of ER-2 and DC-8 aircraft flights over Antarctica, August and September 1987, J. Geophys. Res., 94, 11 181–11 222, 1989. 1991

Urban, J., Lautié, N., Le Flochmoën, E., Jiménez, C., Eriksson, P., De La Noë, J., Dupuy, E., Ekström, M., El Amraoui, L., Frisk, U., Murtagh, D., Olberg, M., and Ricaud, P.: Odin/SMR limb observations of stratospheric trace gases: Level 2 processing of ClO, N_2O, HNO_3, and O_3, J. Geophys. Res., 110, D14307,doi:10.1029/2005JD005741, 2005a. 1984

Urban, J., Lautié, N., Le Flochmoën, E., Jiménez, C., P.Eriksson, De La Noë, J., Dupuy, E., El Amraoui, L., Frisk, U., Jégou, F., Murtagh, D., Olberg, M., Ricaud, P., Camy-Peyret, C., Dufour, G., Payan, S., Huret, N., Pirre, M., Robinson, A. D., Harris, N. R. P., Bremer, H., Kleinböhl, A., Küllmann, K., Künzi, K., Kuttipurath, J., Ejiri, M. K., Nakajima, H., Sasano, Y., Sugita, T., Yokota, T., Piccolo, C., Raspollini, P., and Ridolfi, M.: Odin/SMR limb observations of stratospheric trace gases: Validation of N_2O, J. Geophys. Res., 110, D09301, doi:10.1029/2005JD005394, 2005b. 1984

Urban, J., Murtagh, D., Lautié, N., Barret, B., Dupuy, E., De La Noë, J., Eriksson, P., Frisk, U., Jones, A., Le Flochmoën, E., Olberg, M., Piccolo, C., Ricaud, P., and Rösevall, J.: Odin/SMR limb observations of trace gases in the polar lower stratosphere during 2004–2005, in: Proceedings of the ESA First Atmospheric Science Conference, 8–12 May 2006, Frascati, Italy, edited by: Lacoste, H., Eur. Space Agency Spec. Publ., ESA-SP-628, ISBN-92-9092-939-1, ISSN-1609-042X, 2006. 1984

Wetzel, G., Sugita, T., Nakajima, H., Tanaka, T., Yokota, T., Friedl-Vallon, F., Kleinert, A., Maucher, G., and Oelhaf, H.: Technical Note: Intercomparison of ILAS-II version 2 and 1.4 trace species with MIPAS-B measurements, Atmos. Chem. Phys., 8, 1119–1126, 2008, http://www.atmos-chem-phys.net/8/1119/2008/. 1985

WMO: Scientific assessment of ozone depletion: 2006, Report No. 50, Geneva, 2007. 1979, 1987

Yokota, T., Nakajima, H., Sugita, T., Tsubaki, H., Itou, Y., Kaji, M., Suzuki, M., Kanzawa, H., Park, J. H., and Sasano, Y.: Improved Limb Atmospheric Spectrometer (ILAS) data retrieval algorithm for Version 5.20 gas profile products, J. Geophys. Res., 107, 8216, doi:10.1029/2001JD000628, 2002. 1985

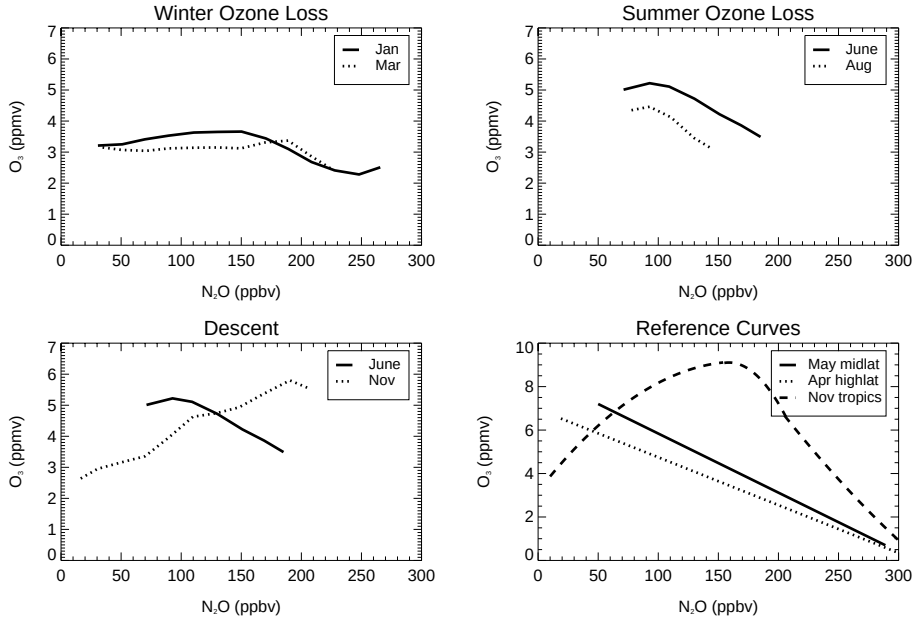

Fig. 1. Schematic of the change of the N_2O and O_3 distribution in the Northern Hemisphere polar region due to photochemical winter ozone loss at 20±2.5 km (top: left) and photochemical summer ozone loss at 25±2.5 km (top: right) and diabatic descent at 25±2.5 km (bottom: left) as well as reference curves (bottom: right) for the midlatitudes (May, ATMOS Shuttle 1985), highlatitudes (April, ATMOS Shuttle 1993) and tropics (November, ATMOS Shuttle 1994). See text for further details.

ACPD
9, 1977–2020, 2009

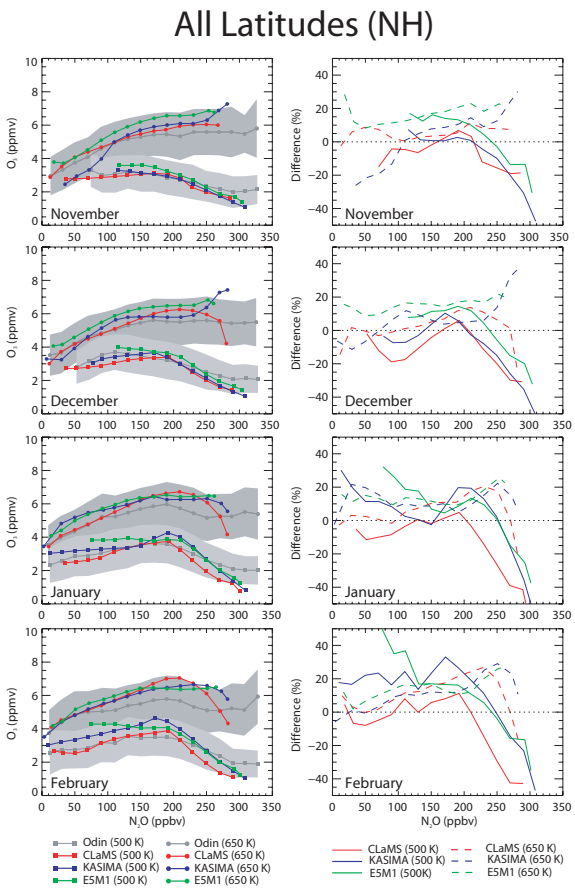

Fig. 2. Left: Comparison of monthly averages of N_2O and O_3 derived from CLaMS, KASIMA and E5M1 (colored curves) with Odin/SMR (grey) at 500±25 K and 650±25 K (Northern Hemisphere). The grey shaded area marks the range of the standard deviations of the monthly averages of O_3 derived from Odin/SMR. Right: Differences of the O_3 averages of CLaMS, KASIMA and E5M1 from Odin/SMR.

ACPD
9, 1977–2020, 2009

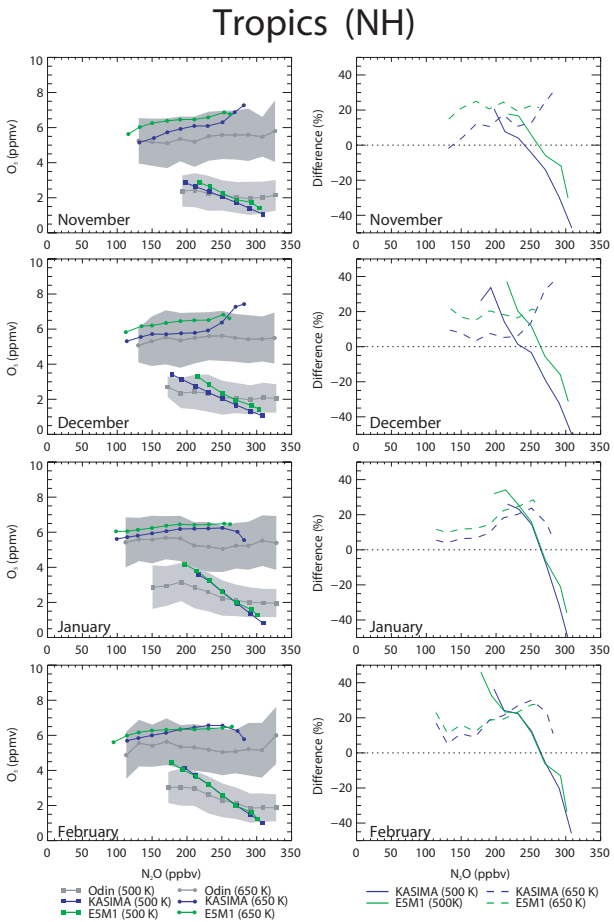

Fig. 3. Left: Comparison of monthly averages of N_2O and O_3 derived from KASIMA and E5M1 (colored curves) with Odin/SMR (grey) at 500±25 K and 650±25 K (Northern Hemisphere tropics). The grey shaded area marks the range of the standard deviations of the monthly averages of O_3 derived from Odin/SMR. Right: Differences of the O_3 averages of KASIMA and E5M1 from Odin/SMR.

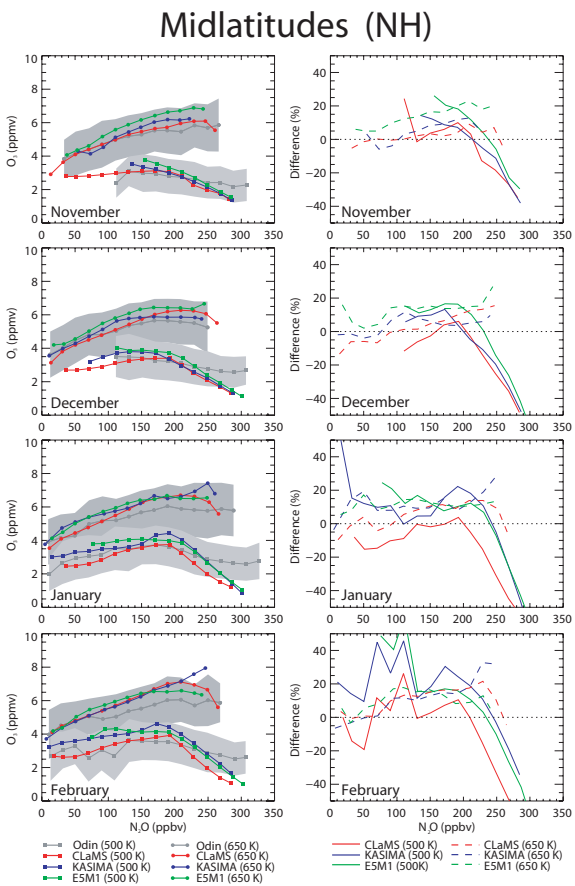

Fig. 4. Left: Comparison of monthly averages of N_2O and O_3 derived from CLaMS, KASIMA and E5M1 (colored curves) with Odin/SMR (grey) at 500±25 K and 650±25 K (Northern Hemisphere midlatitudes). The grey shaded area marks the range of the standard deviations of the monthly averages of O_3 derived from Odin/SMR. Right: Differences of the O_3 averages of CLaMS, KASIMA and E5M1 from Odin/SMR.

ACPD
9, 1977–2020, 2009

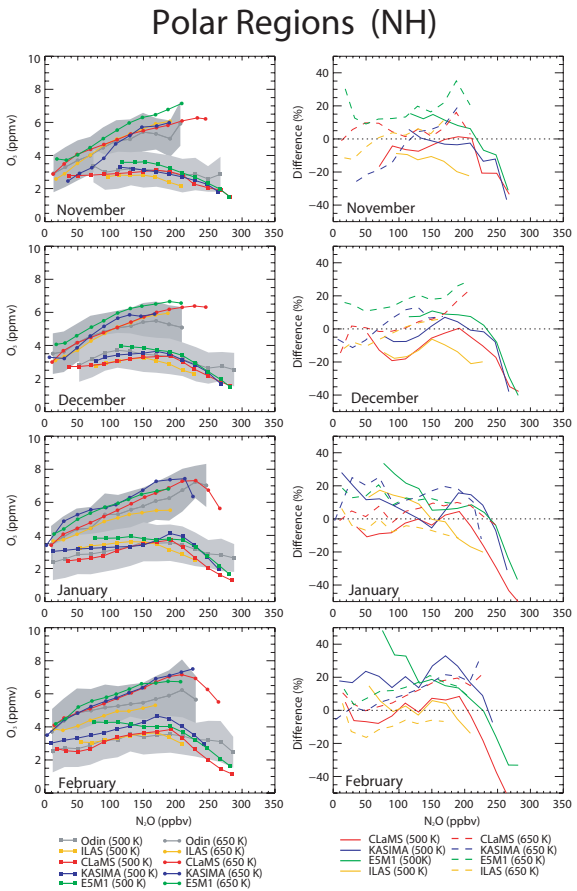

Fig. 5. Left: Comparison of monthly averages of N_2O and O_3 derived from CLaMS, KASIMA, E5M1 and ILAS/ILAS-II (colored curves) with Odin/SMR (grey) at 500±25 K and 650±25 K (Northern Hemisphere polar regions). The grey shaded area marks the range of the standard deviations of the monthly averages of O_3 derived from Odin/SMR. Right: Differences of the O_3 averages of CLaMS, KASIMA, E5M1 and ILAS/ILAS-II from Odin/SMR.

ACPD
9, 1977–2020, 2009

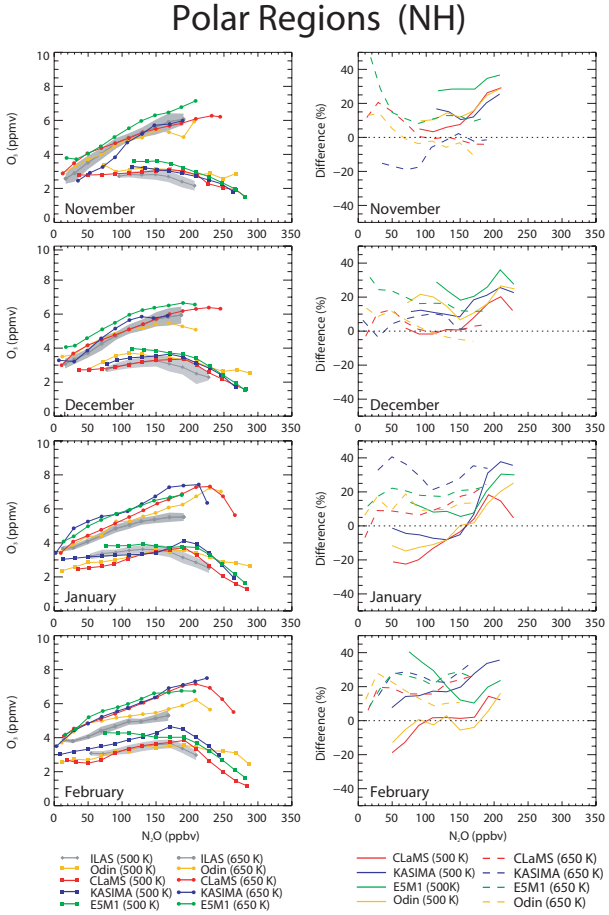

Fig. 6. As Fig. 5, but using ILAS/ILAS-II as reference. Left: Comparison of monthly averages of N_2O and O_3 derived from CLaMS, KASIMA, E5M1 and Odin/SMR (colored curves) with ILAS/ILAS-II (grey) at 500±25 K and 650±25 K (Northern Hemisphere polar regions). The grey shaded area marks the range of the standard deviations of the monthly averages of O_3 derived from ILAS/ILAS-II. Right: Differences of the O_3 averages of CLaMS, KASIMA, E5M1, and Odin/SMR from ILAS/ILAS-II.

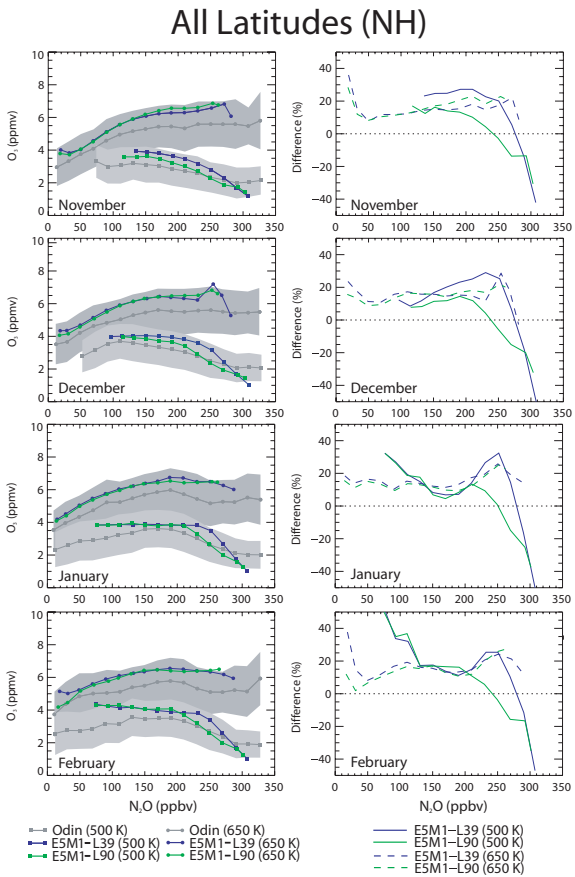

Fig. 7. As Fig. 2, but showing (left) the impact of different vertical resolutions. Left: The comparison of monthly averages of N_2O and O_3 derived from E5M1 T42L90MA and E5M1 T42L39MA simulation (colored curves) with Odin/SMR (grey) at 500±25 K and 650±25 K (Northern Hemisphere). The grey shaded area marks the range of the standard deviations of the monthly averages of O_3 derived from Odin/SMR. Right: Differences of the O_3 averages of E5M1 T42L90MA and E5M1 T42L39MA simulation from Odin/SMR.

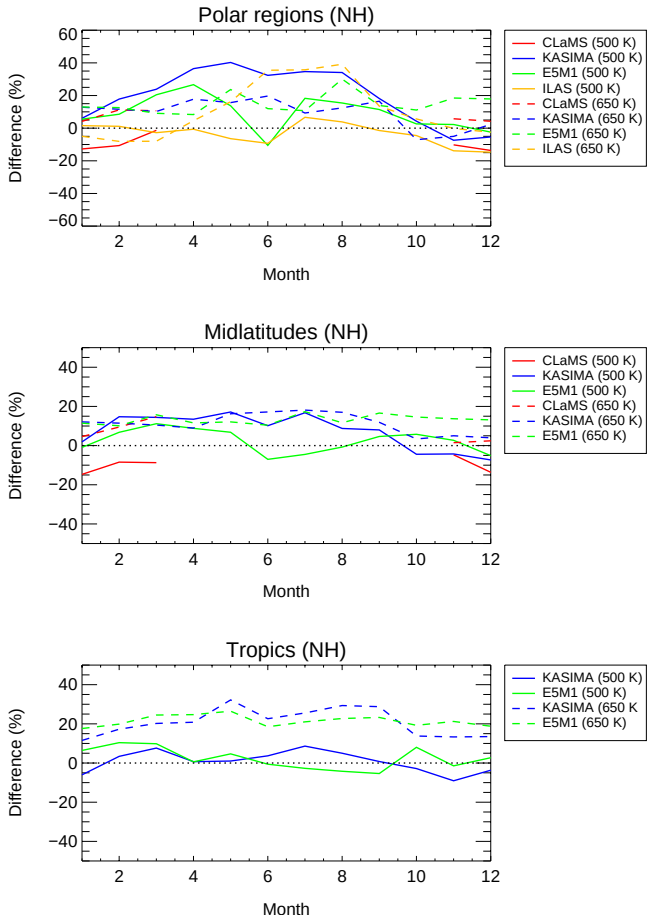

Fig. 8. Averaged differences between the O_3 mixing ratio simulated by the models CLaMS, KASIMA, E5M1 and the O_3 mixing ratios measured by ILAS/ILAS-II from Odin/SMR for every month of the year and separated by latitude region (Northern Hemisphere).

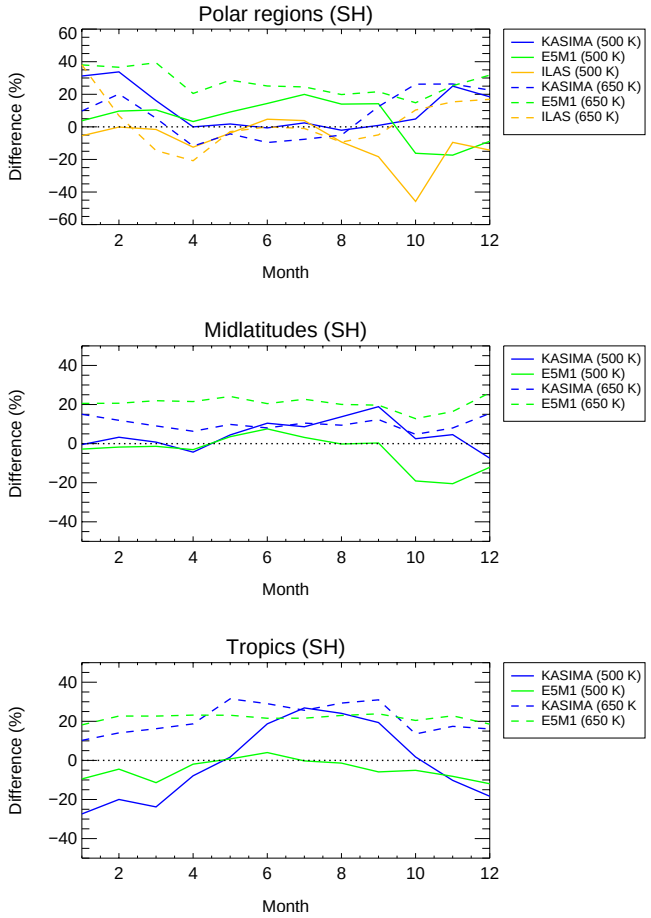

Fig. 9. Averaged differences between the O_3 mixing ratio simulated by the models KASIMA, E5M1 and the O_3 mixing ratios measured by ILAS/ILAS-II from Odin/SMR for every month of the year and separated by latitude region (Southern Hemisphere).